17th World Conference on Earthquake Engineering, 17WCEE
Sendai, Japan - September 13th to 18th 2020

A PREDICTION METHOD OF NON-STRUCTURAL RESPONSE SPECTRA Part 2: Verification of Components in Multi-Story Building

S. Komatsu[(1)], K. Kasai[(2)], and D. Lau[(3)]

[(1)] *Assistant Professor, Shimane University, s.komatsu@riko.shimane-u.ac.jp*
[(2)] *Specially Appointed Professor, Tokyo Institute of Technology, kasai.k.ac@m.titech.ac.jp*
[(3)] *Professor, Carleton University, DavidLau@cunet.carleton.ca*

Abstract

The authors have proposed an improved simplified method to predict responses of non-structural components attached to a single-degree-of-freedom (SDOF) model which represents the *j*-th modal properties of a multi-degree-of-freedom (MDOF) model. The accuracy of the prediction by the proposed method of the non-structural response spectra is verified through comparison with the calculation by time history analysis. Excellent accuracy is observed over extensive variation of parameters (Part 1). This paper presents an expansion of the method to predict seismic response spectra of non-structural component attached to a floor in a MDOF building. The expanded method is based on a combination of the non-structural response spectra using a response spectrum method. In consideration of applying the method up to super-tall buildings, the Complete-Quadratic-Combination (CQC) rule is adopted for the response spectrum method. Investigations using a 30-story building were carried out to clarify response characteristics and prediction accuracy of the non-structural components attached to the middle and near top floor in the super-tall building. The first part of this paper considers a contribution of each modal response component against the non-structural response time history in the 30-story building by use of time history analysis and mode superposition method. In contrast, this second part of the study verifies the prediction accuracy of the non-structural pseudo-acceleration and displacement response spectra in the 30-story building by comparing with spectral solutions obtained from time history analysis.

Keywords: non-structural components; response prediction; response spectra; duration of ground motions; CQC rule

1. Introduction

Part 1 investigates tendencies of time history responses of SDOF non-structural component models attached to a SDOF building model [1]. As a result, the non-structural component shows two different trends: a stationary response when the period of the non-structural component is relatively shorter than that of the building, a non-stationary response directly excited by the seismic ground motion when it is relatively longer. Further, a transfer function to predict the first trend based on a stationary-vibration theory and another transfer function to predict the second behavior trend based on unique ideas from observation obtained from the time history analysis in the frequency domain have led to the derivation of the two prediction formulas, respectively. However, the assumption of the unique ideas in the prediction formula leads to overestimate of the response at the resonance point which depends on the duration of the seismic ground motion and damping ratio of the building and component. Correction coefficients are introduced to reduce the resonance response. Pseudo-acceleration and displacement spectra of the components in SDOF building models can be generated over an extensive range of natural period, damping ratio of the building and components, and 16 earthquake ground motion records with various spectral characteristics and the duration. The typical spectral shapes and the prediction accuracy of the proposed method are discussed.

On the premise of the above, this paper discusses the estimation of the response of non-structural components in a multi-degree-of-freedom (MDOF) building model. To predict the response of the components in the MDOF building models, it is essential to understand that the non-structural components

excited by the various building modal responses and contributions of these responses are different at each building floor. As mentioned in Part 1, some previous generation methods are applicable for the non-structural components in the MDOF building models [2 to 4], although these studies have not investigated the behavior trend of the non-structural response time history in a MDOF building model and their contributions of modal responses to the total response.

The purpose of this study is to expand the improved simplified method to consider non-structural components in MDOF building models, to verify its prediction accuracy. In section 2, the contribution of each modal response to the non-structural response time history is evaluated by superpositioning the time history responses of the SDOF component model excited by the SDOF building model which represents the individual modal response in a 30-story building. In section 3, a modification to the Complete-Quadratic-Combination (CQC) rule is proposed to predict the maximum response of non-structural components in a multi-story buildings. Using 16 earthquake records, the pseudo-acceleration and displacement spectra at the middle and near top story in the 30-story building are generated with excellent accuracy.

2. A consideration on response behavior of non-structural components in buildings

In part 1, the SDOF building models with natural period T_{bj} = 0.5, 2, and 5s are considered. In the first part of this section here, in contrast, the SDOF building models are obtained from the modal properties of a 30-story building.

2.1 Outline of 30-story building model

The j-th mode natural period T_{bj}, damping ratio h_{bj}, and participation vectors at the 15th and 28th floor $\beta_j\phi_{15j}$, $\beta_j\phi_{28j}$ for j = 1 to 8 mode are shown in Table 1. Two cases of proportional Rayleigh damping are considered: $h_{b1} = h_{b2} = 0.02$ (low-damping) and $h_{b1} = h_{b2} = 0.1$ (high-damping).

Table 1 – Properties of 30-story building

Mode order j		**1**	**2**	**3**	**4**	**5**	**6**	**7**	**8**
T_{bj} (s)		3.01	1.18	0.720	0.537	0.432	0.361	0.306	0.267
h_{bj}	**$h_{b1} = h_{b2} = 0.02$**	0.020	0.020	0.027	0.034	0.041	0.049	0.057	0.065
	$h_{b1} = h_{b2} = 0.1$	0.100	0.100	0.135	0.171	0.207	0.243	0.284	0.324
$\beta_j\phi_{ij}$	**15th story**	0.680	0.453	0.085	-0.132	-0.157	-0.057	0.083	0.091
	28th story	1.378	-0.547	0.230	-0.022	-0.131	0.180	-0.156	0.107

Fig. 1 shows $\beta_j\phi_{4j}$, $\beta_j\phi_{15j}$, and $\beta_j\phi_{28j}$ from j = 1 to 30 as a typical example of the participation vectors at representative floors in the super-tall building. In the lower-part of the building, the same sign is continuing from the low-order mode and an absolute value of the high-order mode takes relatively greater value. In contrast, in the higher-part of the building, the sign changes in different modes and the absolute values of the lower modes are greater than that of the higher modes.

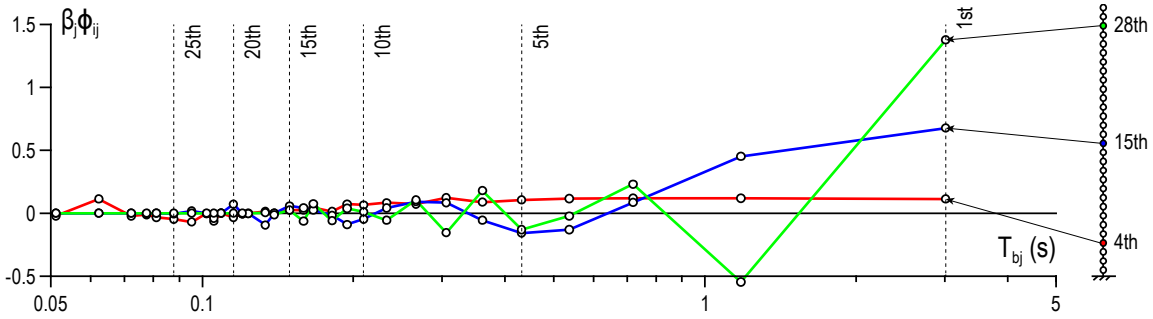

Fig. 1 – Participation vectors at representative floor in 30-story building

2.2 Modal response of multi-story building and non-structural components

Fig. 2 shows the time history of absolute acceleration response $\ddot{X}_j(t) + \ddot{u}_g(t)$ calculated by using the SDOF building models subjected to Hachinohe EW. Here, the SDOF model has the j-th modal properties of the 30-story building ($h_{b1} = h_{b2} = 0.02$). The vibration periods T_{bj}' for j = 1 to 8 corresponding to mode 1 to mode 8 are also shown in Fig. 2a. Fig. 2b shows eight time histories of j = 9 to 30 with increment of three. The response $\ddot{X}_j(t) + \ddot{u}_g(t)$ are similar to $\ddot{u}_g(t)$ when j is greater than 9, and it approaches $\ddot{u}_g(t)$ shown by the gray thick line in more higher mode. A correlation coefficient of the 9th mode building response $\ddot{X}_9(t) + \ddot{u}_g(t)$ against $\ddot{u}_g(t)$ is taken as $\rho = 0.63$, and it satisfies the threshold value of the rigid mode $\rho = 0.5$ in Reference [5]. From the same analytical investigations by using the other two seismic waves, larger than 9th mode response of the SDOF building is considered as the rigid mode.

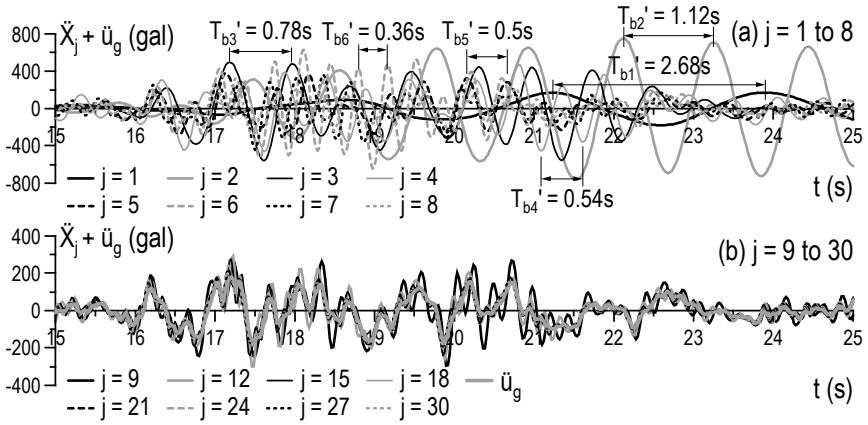

Fig. 2 – Absolute Acceleration response of j-th mode SDOF models (Hachinohe EW)

Fig. 3 shows time history solution of absolute acceleration response $\ddot{X}_j(t) + \ddot{Y}_j(t) + \ddot{u}_g(t)$ calculated by using the SDOF non-structural component ($T_c = 0.3$s, $h_c = 0.02$) subjected to $\ddot{X}_j(t) + \ddot{u}_g(t)$ (Fig. 2). The acceleration response of the non-structural component is similar to that of the j-th mode building when the non-structural components are relatively stiffer than the building at j = 1 to 6 ($T_{b6} = 0.361$s), and the response is amplified when T_c and T_{bj} are close at j = 7 and 8 (Fig. 3a). The response shows a tendency of directly subjected to the seismic ground motion when the components are relatively softer than the building at j = 9 ($T_{b9} = 0.233$s) to 30 (Fig. 3b). Further, for more longer period T_c = 2s, the similar acceleration to the building and the similar acceleration to the case of directly excited by the ground motion were observed at j = 1 to 2 and j = 3 to 30, respectively.

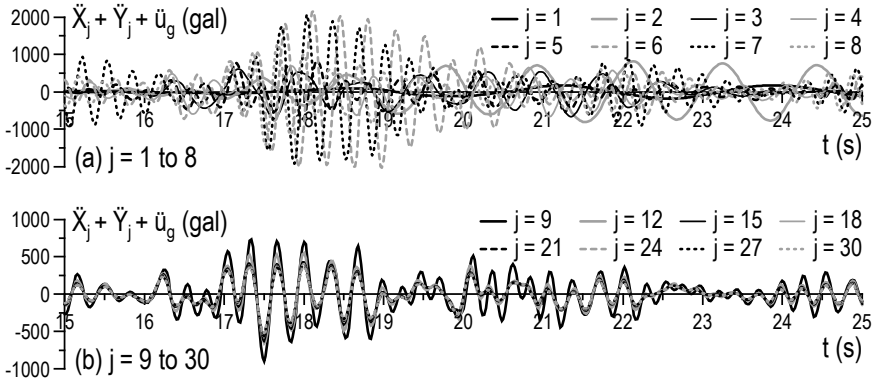

Fig. 3 – Absolute Acceleration response of j-th mode SDOF models (Hachinohe EW)

2.3 Contribution of modal responses to non-structural response

Fig. 4a shows the absolute acceleration of the non-structural components with T_c = 0.3s and h_c = 0.02 at the 28th floor in the 30-story building. Here, "j = 1 to 8" or "j = 9 to 30" is obtained by superposition of $\ddot{u}_{c,tot,28j}(t)$ (multiplication of $\beta_j\phi_{28j}$ and $\ddot{X}_j(t) + \ddot{Y}_j(t) + \ddot{u}_g(t)$) for $j = m$ to n, and "Analysis" is the accurate time history solution directly obtained from time history analysis of the 30-story building and the SDOF component. The maximum value and phase of the accurate solution are determined based on mode superposition of the responses of j = 1 to 8. In contrast, the maximum value of the mode superposition result from j = 9 to 30 against that of the accurate solution is only 4.6% because the adjacent modal response components are canceled out due to the sign of $\beta_j\phi_{28j}$. Also, in the case of the non-structural component with T_c = 2s and h_c = 0.02, the maximum value and phase are obtained by mode superposition of the responses of j = 1 to 2, the contribution of j = 3 to 30 is quite small (Fig. 4b).

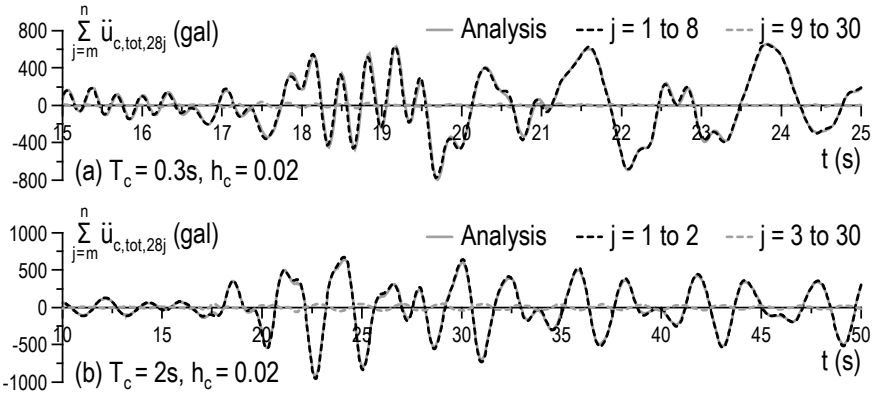

Fig. 4 – Absolute acceleration responses of components at 28th floor (Hachinohe EW)

For T_c = 0.1s, the superposition method requires to take the same number of modes as the building (i.e., j = 1 to 6 for Hachinohe EW and the 28th floor) for reproducing the accurate solution because the non-structural component moves same as the building floor. Whereas, for T_c = 5s, the method requires to take j = 1 to 2. Furthermore, the accurate solution of the non-structural components at the 15th floor can be reproduced with the same number of modes as the 28th floor, since the sign of $\beta_j\phi_{15j}$ switches in different modes and the absolute value at the lower mode is dominant in almost the same as the response at the 28th floor. The above trends are common to not only Hachinohe EW but JMA Kobe NS, Tomakomai EW, and combination cases of the damping ratio $h_{b1} = h_{b2}$ = 0.02, 0.1 and h_c = 0.02, 0.1.

From the above, the required number of modes to reproduce time history response is determined by characteristics of the ground motion, relation between the natural period of the building and component, and the absolute value and sign of the participation vector. To reproduce time history response of the components with T_c = 0.1, 0.3, 2, and 5s at the 15th and 28th floor in the 30-story building model, it is necessary to combine the maximum modal responses up to the 8th mode.

3. Response prediction of SDOF non-structural components in multi-story building

3.1 Non-structural response spectra subjected to modal building response

In this section, instead of the mode superposition method the spectrum method is employed to combine $S_{pac,j}(T_c, h_c)$ for j = 1 to n, with simplification, where n is the mode order less than the degree-of-freedom of the multi-story building.

The spectrum method for the buildings combines the j-th modal maximum building response from j = 1 to n.

In contrast, the method for the non-structural components utilizes the maximum response of the components subjected to the *j*-th mode building response. Because of this difference, the square-root-of-sum-of-square (SRSS) method and CQC rules currently used for the building response prediction are substituted to predict the response of the components as Equation (1) and (2), respectively.

$$S_{pac}(T_c, h_c)(i\text{-th}) = \sqrt{\sum_{j=1}^{n} \{\beta_j \phi_{ij} S_{pac,j}(T_c, h_c)\}^2} \tag{1}$$

$$S_{pac}(T_c, h_c)(i\text{-th}) = \sqrt{\sum_{j=1}^{n}\sum_{k=1}^{n} \rho_{jk} \beta_j \beta_k \phi_{ij} \phi_{ik} S_{pac,j}(T_c, h_c) \cdot S_{pac,k}(T_c, h_c)}$$

$$\rho_{jk} = \frac{8\sqrt{h_{bj} h_{bk}}\,(\alpha h_{bj} + h_{bk})\alpha^{\frac{3}{2}}}{(\alpha^2 - 1)^2 + 4h_{bj}h_{bk}\alpha(\alpha^2 + 1) + 4(h_{bj}^{\,2} + h_{bk}^{\,2})\alpha^2} \tag{2a, b}$$

where *j*, *k* = mode order, ρ_{jk} = correlation coefficient, and $\alpha = \omega_{bj} / \omega_{bk}$.

In the case of S_{pac}(28th) (T_c, $h_c = 0.02$) with $h_{b1} = h_{b2} = 0.1$ and JMA Kobe NS, there is clear difference between the two combination methods as shown in Fig. 5a, b. The SRSS method and CQC rules with n = 5 to 8 (8 is the necessary mode number to reproduce the accurate solution for T_c = 0.1, 0.3, 2, and 5s, section 2.3) are compared with the accurate spectral solution. Further, reducing the response at the resonance point by γ_{bj} is not considered for $h_{bj} > 0.1$ whereit is out of the applicable range for the equation of γ_{bj}. This makes the estimate of the response on the conservative side.

The difference between the two combination methods is shown notably when T_c is less than the 3rd mode building natural period (T_{b3} = 0.72s, Table 1). The SRSS method, which simply sums of squares of each modal response, does not take into account the sign of the participation vector, and therefore it leads to an overestimate of the response which increases with n increases. For these observations and the time history results, n = 8 is adopted for the CQC rules (Equation 2).

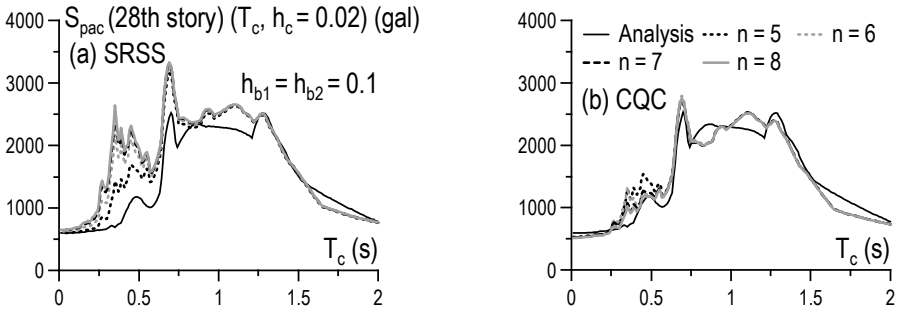

Fig. 5 – Comparison between SRSS and CQC (JMA Kobe NS)

3.2 Response prediction procedures of the proposed method

This method requires to know the modelling properties as follows: the *j*-th participation vector $\beta_j \phi_{ij}$, natural period T_{bj}, damping ratio h_{bj} of the multi-story building, the damping ratio of the SDOF component model h_c, and the ground acceleration motions for the seismic response spectrum and the earthquake ground motion duration t_d. The response prediction procedures to generate the non-structural pseudo-acceleration and displacement spectrum at the *i*-th story in a multi-story building S_{pac},S_{dc}(*i*-th) (T_c, h_c) can be summarized in the following steps. Here T_c is a variable parameter. In this section, the equation numbers in Part 1 and 2 are distinguished to add "1" or "2" to the lead of the numbers.

1) By using building pseudo-acceleration spectrum $S_{pa}(T, h)$, calculate $S_{pa}(T_{bj}, h_{bj})$ and $S_{pa}(T_{bj}, h_c)$ values. Also, rewritng $S_{pa}(T, h_c)$ as $S_{pa}(T_c, h_c)$.

2) By utilizing the above $S_{pa}(T_{bj}, h_{bj})$ and $S_{pa}(T_{bj}, h_c)$, obtain the j-th mode correction term A_j from Equation (1.11) and B_j from Equation (1.14b). Further, determine correction coefficient γ_{bj} by Equations (1.12), (1.13) and γ_c by Equation (1.14a).

3) From prediction formula 1 and $S_{pa}(T_{bj}, h_{bj})$, generate $S_{pac,j}(T_c, h_c)$ curve by Equation (1.6).

4) From prediction formula 2 and $S_{pa}(T_{bj}, h_c)$, generate $S_{pac,j}(T_c, h_c)$ curve by Equation (1.10).

5) Determine the bigger value at each T_c from procedure 3) and 4) as the j-th mode prediction value $S_{pac,j}(T_c, h_c)$. Obtain $S_{pac}(i\text{-th})(T_c, h_c)$ by combining the modal responses of $S_{pac,j}(T_c, h_c)$ and the correlation coefficients ρ_{jk} from $j = 1$ to n by the CQC rules in Equation (2.2), and then multiply that by $(T_c / 2\pi)^2$ to get $S_{dc}(i\text{-th})(T_c, h_c)$.

3.3 Response prediction of non-structural components at middle- and high-story floor

Fig. 6a to c shows the pseudo-acceleration spectra of the non-structural components at the 15th and 28th floor $S_{pac}(15\text{th})(T_c, h_c)$, $S_{pac}(28\text{th})(T_c, h_c)$ obtained from Equation (2) ($n = 8$) and comparison with theaccurate solutions. The accurate solution is defined as the pseudo-acceleration spectrum of the SDOF non-structural component model subjected to the building response at target floor directly obtained from the time history analysis of the 30-story building. Three input earthquake motions are considered: the JMA Kobe NS, Hachinohe EW, and Tomakomai EW.

Generally, the response spectra $S_{pac}(i\text{-th})(T_c, h_c)$ at the middle- or high-story floor have the typical behaviorwith a peak at each T_{bj}. These peak values which depend on the floor are due to the difference between participation vectors, e.g., the peak of the 4th mode appears at the 15th floor and not at the 28th floor. Further, high damping ratio of the component reduces the peak response at the resonance point, where it does not have much effect in the concave part of the curves shown in Fig. 6. Hence, it is necessary to increase the building damping ratio h_{bj} for reduction of the non-structural response spectra over the whole period range.

For the 15th and 28th floor, the prediction accuracy of the peak response around each T_{bj} depends on that of γ_{bj} corresponding to each mode. For example, in the case of JMA Kobe NS and $T_{b1} = 3.01$s, the prediction at the 1st mode period overesimates the actual value because of the predicted γ_{b1} is influenced by a short-period pulse motion. This is the same reason of Sylmar and $T_{bj} = 5$s (Appendix, Part 1), although this case was not as excessive as the Sylmar. Fig. 7 shows the ratio obtained by dividing the predicted value by the accurate solution value, and its mean value and coefficient of variation for 500 points in the range of $T_c = 0.01$ to 5.00s (500 points). Also, Table 2 shows the mean value and standard deviation for 16 seismic ground motions. The CQC rules can predict the non-stuctural response spectrua at the middle- and high-story for various seismic excitations with good accuracies. However, it should be noted that the error of γ_{bj} possibly causes the decrease in the prediction accuracy as mentioned above.

Fig. 8 shows the non-structural displacement spectra $S_{dc}(28\text{th})(T_c, h_c = 0.02)$ obtained from multiplying $S_{pac}(28\text{th})(T_c, h_c = 0.02)$ by $(T_c / 2\pi)^2$. The 1st mode resonance response in the pseudo-acceleration spectra is relatively smaller than that of the 2nd mode, but the most predominant displacement occurs at the 1st mode resonance points (Fig. 8).

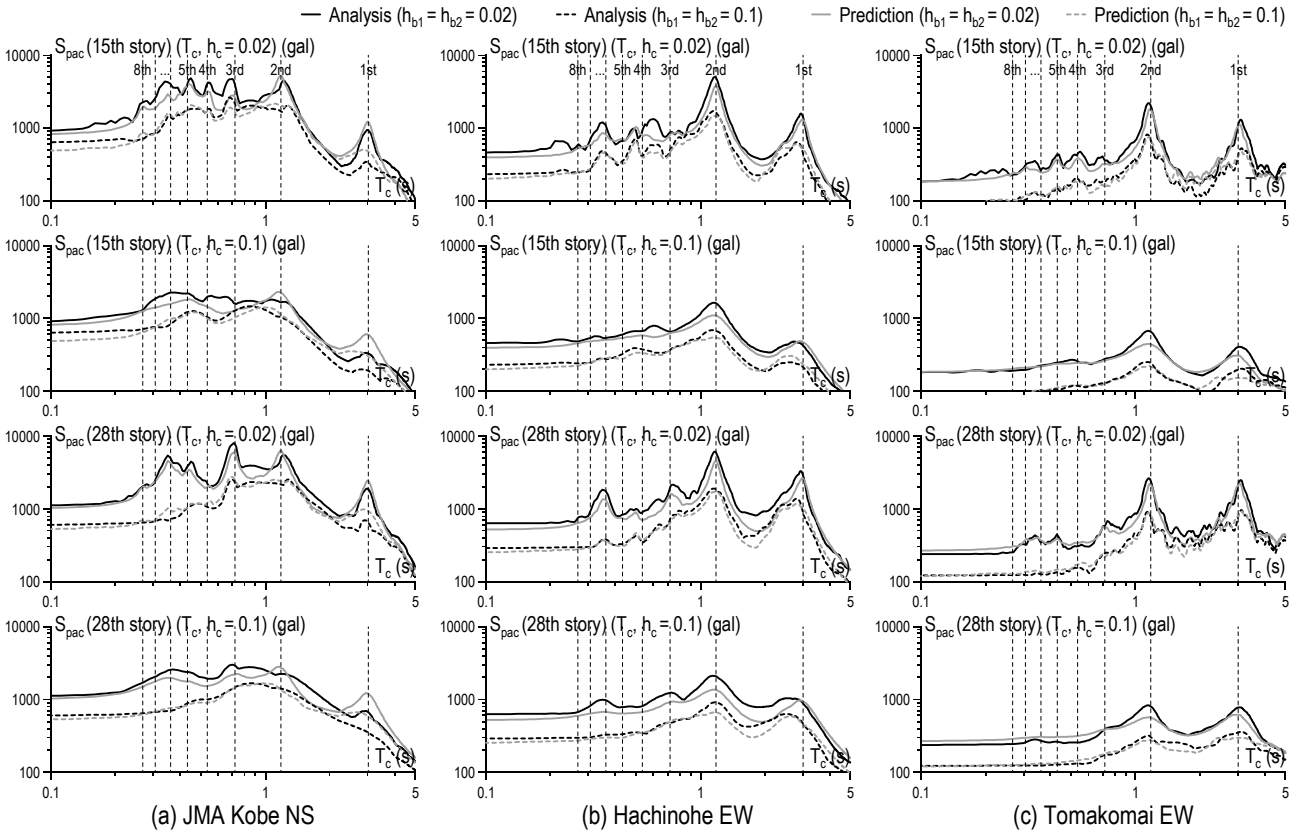

Fig. 6 – Analysis vs. prediction: pseudo-acceleration spectra of components
(15th and 28th story in 30-story building model)

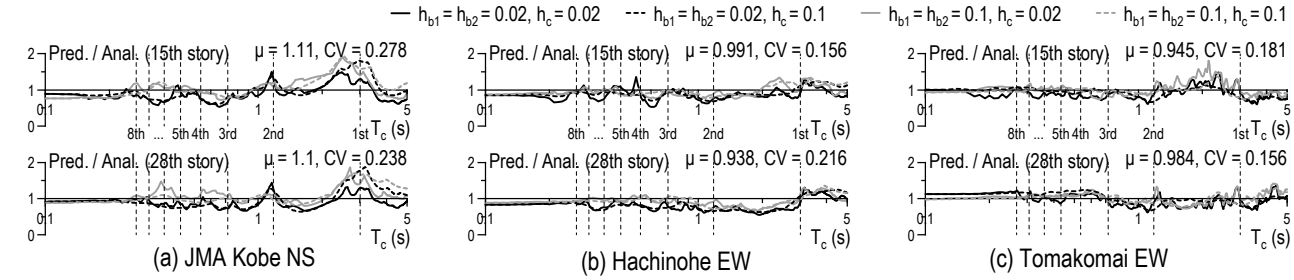

Fig. 7 – Prediction accuracies of MDOF models
(μ = mean value for T_c = 0.01 to 5s, σ = standard deviation, CV = σ / μ)

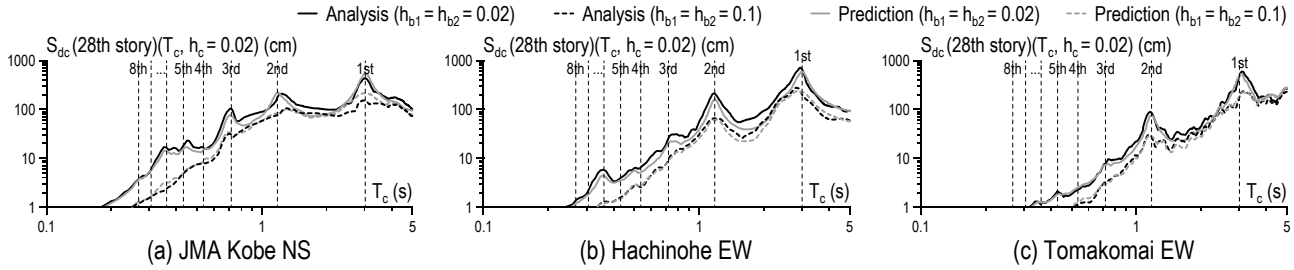

Fig. 8 – Analysis vs. prediction: displacement spectra of components
(15th and 28th story in 30-story building model)

3.4 Response prediction of non-structural components at low-story floor

Damage to the non-structural components at the low-story floor in the building is assumed to be small because the non-structural response does not amplify compared with the high-story floor. However, it is important to grasp the difference between the prediction of the lower- and higher-floor for promotion of understanding the method, so that we provide some considerations here. In the case of Tomakomai EW used as input to the 30-story building with $h_{b1} = h_{b2} = 0.02$, the accurate solution of the non-structural spectra $S_{pac}(i\text{-th})$ (T_c, $h_c = 0.02$) at $i = 1$ to 10 story and their prediction obtained from the CQC rules ($n = 8$) are shown in Fig. 9.

The similarity of $S_{pac}(1\text{st})$ (T_c, h_c) and the seismic response spectrum $S_{pa}(T_c, h_c)$ is attributed to almost the same vibrations of the 1st floor and ground. The peaks on the spectral curve clearly appear at each T_{bj} because the effects of the building response become stronger in high-story floor (Fig. 9). The prediction values are significantly less than the accurate solution at the more low-story floor, but these approaches the accurate solution as it becomes more high-story floor. Also, the prediction value obtained from the CQC rules ($n = 8$) was almost matched with the accurate solution from $i = 7$. This is due to, the contribution of the participation vector of more high-order mode becomes dominant at the low-story floor, and the response spectrum method requires more high-order mode for high accuracy prediction. However, since it is practically difficult and time-consuming to consider many modes, it is suggested to use the prediction value of higher story floor than the target floor.

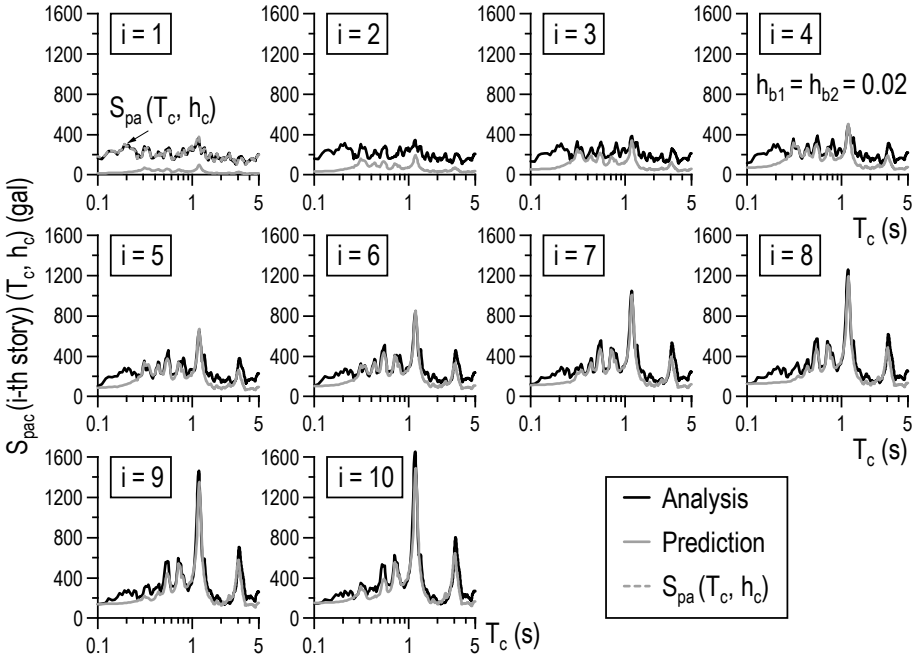

Fig. 9 – Pseudo-acceleration spectra at lower floors (Tomakomai EW)

4. Conclusion

The contribution of each modal response to the non-structural components attached to the middle- and near top story in a 30-story building model is investigated using time history analysis. Then, an extension of the prediction method discussed in Part 1 is proposed to evaluate the response of non-structural components attached to the building floors in MDOF buildings. The accuracy of the prediction of maximum acceleration and displacement at the middle- and near top floor in the 30-story building is presented. Significant conclusions can be summarized as follows.

1) The superposition of the time history responses of the SDOF non-structural component models subjected to each vibration modal response has been carried out. From observations, the required number of mode order to reproduce time history response depends on the characteristics of the ground motion, relation between the natural period of the building and non-structural components, and the absolute value and sign of the participation vector.

2) Using CQC rules, the non-structural pseudo-acceleration spectral curves can be obtained from the combination of each spectral curves, which are generated by the method of Part 1 based on the natural period and damping ratio of the modal properties of the building. Also, the non-structural displacement spectra is obtained by simple transformation of the results. Excellent prediction accuracy is observed by the combination of modes 1 to 8 at the middle- and high-floor in the 30-story building.

5. References

[1] Kasai K, Komatsu S, Lau D (2020): A Prediction Method of Non-Structural Response Spectra, Part 1: Outline of Prediction Method and Verification with SDOF Building, *17WCEE*, Sendai, JAPAN.

[2] Ishihara T, Sato K, Suzuki K, Nagano M (2017): Proposal of a Direct Estimation Method for Floor Response Spectrum in Non-linear Seismic Behavior, *AIJ Journal of Technology and Design*, **54** (23), 433-436.

[3] Yasui Y, Yoshihara J, Takeda T, Miyamoto A (1993): Direct Generation Method for Floor Response Spectra, *Proceedings of the 12th International Conference SMiRT*, K13/4, 367-372.

[4] Jiang W, Li B, Xie W, Pamdey MD (2015): Generate Floor Response Spectra: Part 1. Direct Spectra-to-Spectra Method, *Nuclear Engineering and Design*, **293**, 525-546.

[5] Kasai K, Motoyui S, Ooki Y (2002): A Study on Application of Viscoelastic Dampers to a Space Frame and Response Characteristics Under Horizontal Ground Motions, AIJ Journal of Structural and Construction Engineering, **561**, 125-135.

[6] Kasai K, Komatsu S, Kondo S, Akatsuka N (2019): Seismic Response Spectrum Rule for Non-Structural Components in Buildings, *AIJ Journal of Structural and Construction Engineering*, **758** (84), 489-499.

